Chin. Sci. Bull. (2014) 59(34):4823–4828
DOI 10.1007/s11434-014-0601-2

csb.scichina.com

Article

Geochemistry

The long-term denudation rate of granitic regolith in Qinhuangdao, North China determined from the in situ depth profile of the cosmogenic nuclides ^{26}Al and ^{10}Be

Lifeng Cui · Congqiang Liu · Sheng Xu · Zhiqi Zhao · Chenglong Tu · Taoze Liu · Hu Ding

Received: 19 May 2014 / Accepted: 7 July 2014 / Published online: 16 August 2014

Abstract This study quantifies the surface denudation rate of granitic regolith via the application of the in situ cosmogenic ^{26}Al and ^{10}Be depth profile in China. The concentration ranges of ^{26}Al and ^{10}Be in the quartz along the ~3-m granitic regolith profile in Qinhuangdao are (4.9–23.1) × 10^5 and (2.3–36.6) × 10^4 atoms/g, respectively. With the exception of the surface sample, both ^{26}Al and ^{10}Be concentrations decrease exponentially with sample depth. The *Chi*-square best-fitting results revealed a total denudation rate of ~9 m/Ma averaged over a 10^3–10^5 a timescale, which is lower than the values observed in global granitic outcrops. Compared with global datasets, the flat terrain due to the lack of tectonic activities is most likely the dominant factor that controls the local denudation process. The surface sample offsets from the theoretical cosmogenic nuclide distribution implies that the denudation rate from river basin sediment could be overestimated because of the bioturbation in the surficial soil layer.

Keywords Weathering rate · Physical erosion · Soil erosion · Carbon cycle · Climate change

L. Cui · C. Liu (✉) · Z. Zhao · C. Tu · T. Liu · H. Ding
State Key Laboratory of Environmental Geochemistry, Institute of Geochemistry, Chinese Academy of Sciences, Guiyang 550002, China
e-mail: liucongqiang@vip.gyig.ac.cn

L. Cui
University of Chinese Academy of Sciences, Beijing 100049, China

S. Xu
Scottish Universities Environmental Research Centre, Glasgow G75 0QF, UK

1 Introduction

Surface denudation rate quantification is one of the basic subjects of study regarding the role that rock weathering plays in the global carbon cycle and the evolution of local landscapes. However, no appropriate method existed to directly estimate denudation rate using a time scale of 10^3–10^5 until accelerator mass spectrometry (AMS) was improved in the 1980s. Compared with conventional methods, the application of in situ terrestrial cosmogenic nuclides (TCNs) has advantages because it records the history of long-term erosion and can minimize the uncertainty caused by the extrapolation problems that other methods must consider [1]. In situ TCNs (i.e., ^{26}Al, ^{10}Be and ^{36}Cl, which have half-lives of 0.71, 1.39 Ma and 301 ka, respectively) are produced in earth surface mineral grains by secondary cosmic rays that can penetrate a few meters underground, and they have been widely applied to directly determine exposure age and denudation rate for approximately 20 years [1, 2]. Importantly, TCN depth profiles provide a highly accurate method for quantifying the long-term denudation rates of unconsolidated surfaces [2, 3]. Long-term denudation and fluvial incision rates determined using these depth profiles have been reported for a variety of climatic, topographic, lithological and tectonic environments [4–6]. Although previous studies have been conducted in China, including estimations of the erosion rates of the Yangtze River catchment using in situ ^{10}Be from modern river sediments [7] and the bedrocks in northern Tibet using the surface ^{10}Be–^{26}Al pair [8], few previous studies have applied the ^{10}Be–^{26}Al pair depth profile to China's geology. Because granitic rocks are widely distributed throughout China and contain abundant quartz (which is the ideal target mineral for preserving in situ cosmogenic nuclides), we sought to apply this depth profile to quantify the denudation rate of granitic regolith due to physical erosion and chemical

weathering and clarify the major factors that control the denudation process. The current paper reports the ^{10}Be and ^{26}Al results from a granitic regolith profile near Qinhuangdao, North China.

2 Methods and materials

2.1 Geological setting

The studied site is located south of Qinhuangdao (119°31.70′E, 39°54.29′N; Fig. 1). Climatically, this site is located in a warm temperate zone and features an oceanic semi-humid climate with a mean annual precipitation (MAP) of 645.9 mm and a mean average temperature (MAT) of 10.5 °C. The granitic regolith, which is located 25 m above sea level, formed in a coastal plain environment (1.5 km from the present coastal line) without a shielding effect and was produced during the Pliocene epoch. Tectonically, the research area is part of the Shanhaiguan anticline in the Sino-Korean paraplatform. Neoarchean microcline granite with a ^{207}Pb/^{206}Pb age of approximately 2,500 Ma composes the bedrock underlying the regolith [9, 10]. Thus, few inherited cosmogenic nuclides ^{26}Al and ^{10}Be existed. However, the local plain landform formed after the Eogene, and the second level planation surface formed during the Neogene period. Based on the geological evidence of the local river, marine terraces and multilayer karst caves, intermittent uplift was characteristic of the tectonic activities during the Quaternary, which indicates that the granite regoliths have not been buried since their first surface exposure [11]. The mean uplift rate in Qinhuangdao is 0.15 mm/a over the past 5 ka [12]. The local climatic conditions suggest a minimal effect of snow shielding and glacier cover on in situ cosmogenic nuclides because the amount and period of annual snow accumulation are not significant.

2.2 Sampling and chemical preparation

Six granitic regolith samples were collected at various depths at intervals of approximately 50 cm along a ~3 m regolith profile (Fig. 2). Care was taken to judge non-disturbance due to human activities.

The samples were first crushed and then sieved to obtain a grain size fraction between 0.25–0.50 mm, which was used for ^{10}Be and ^{26}Al preparation and measurement. Quartz purification was conducted at the State Key Laboratory of Environmental Geochemistry at the Institute of Geochemistry, Guiyang. The magnetic minerals in the rock samples were eliminated using a magnetic separator. The quartz was then purified using the chemical etching method [13]. This etching process was repeated several times to remove surficial meteoric ^{10}Be and any other silicate minerals. The purity of the quartz was repeatedly assessed based on the ^{27}Al concentration in the samples, which was

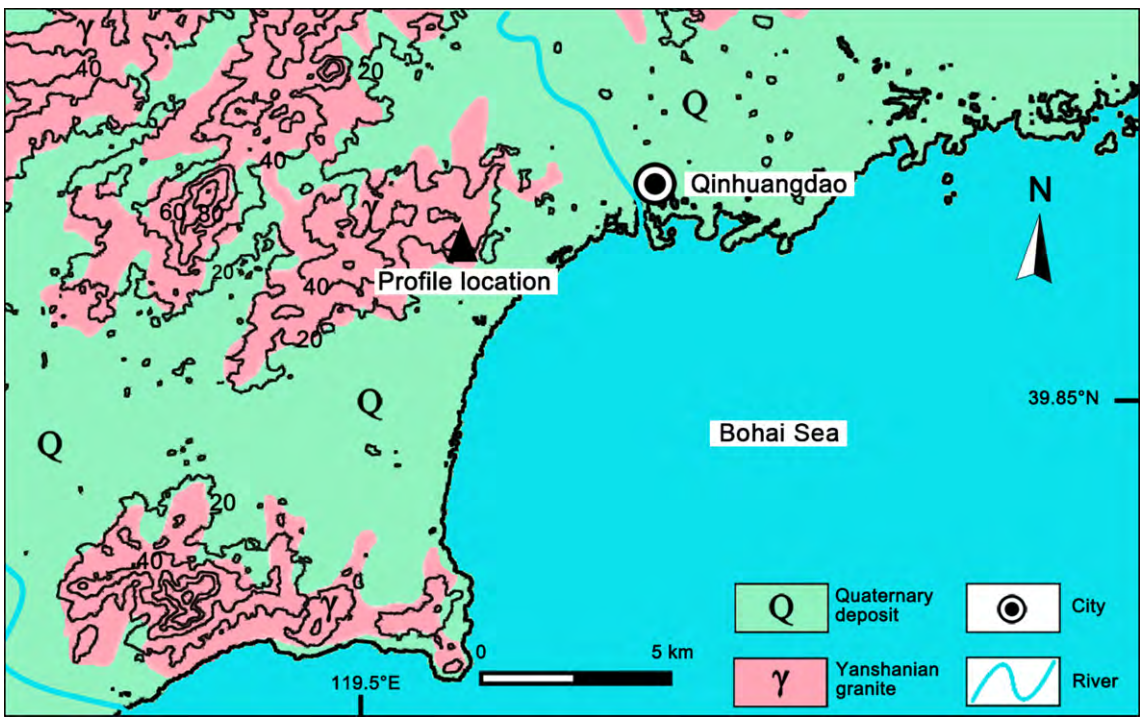

Fig. 1 Geological and contour map showing lithology and topography for sampling site

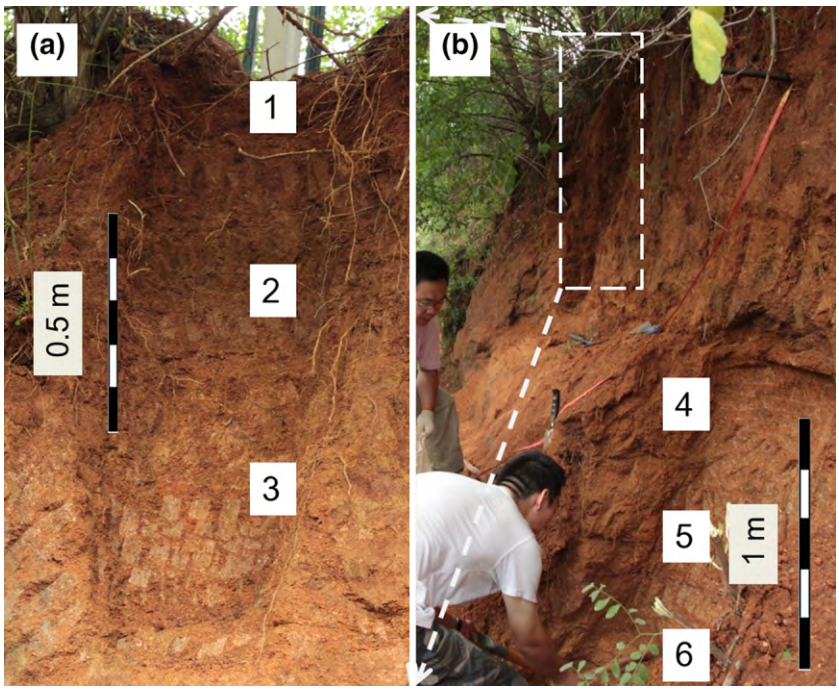

Fig. 2 Photos showing samples distribution on the profile. **a** The upper layer: 0–160 cm; **b** the lower layer: 160–300 cm

determined by an aliquot of samples using inductively coupled plasma optical emission spectrometer (ICP-OES).

Extractions and measurements of ^{26}Al and ^{10}Be were conducted at the Scottish Universities Environmental Research Centre (SUERC). The purified quartz was spiked with ^{9}Be carrier at known concentrations (and ^{27}Al in cases of low concentrations) and then dissolved with concentrated hydrofluoric acid. This step was followed by an anion and cation exchange with a series of column chromatography. The pH of the solution was adjusted to obtain $Be(OH)_2$ and $Al(OH)_3$ precipitation. Finally, the precipitated $Be(OH)_2$ and $Al(OH)_3$ were oxidized into BeO and Al_2O_3. A blank sample with ^{9}Be and ^{27}Al carrier was created following the same procedure as the unknowns. For the AMS measurement, BeO and Al_2O_3 were mixed with Nb (BeO:Nb = 1:6 w/w) and Ag (Al_2O_3:Ag = 1:2 w/w) powder, respectively, and pressed in a Cu sample holder with a 1 mm diameter. The ^{10}Be/^{9}Be and ^{26}Al/^{27}Al ratios were determined using the SUERC 5 MV AMS facility at terminal conditions of 5 and 4 MV, respectively. Details of the instrumental conditions and data reduction can be found in Xu et al. [14].

2.3 Denudation rate calculation

Three mechanisms produce the cosmogenic nuclides ^{26}Al and ^{10}Be: high-energy spallation, negative muon capture and fast muon interactions [15]. We calculated the production rate due to spallation using the scaling scheme of Stone [16] and Lal [5] as well as the production due to negative muon capture and fast muon interactions according to Heisinger et al. [17, 18]. The resulting total surface production rates were 4.2 atoms/g a for ^{10}Be and 28.8 atoms/g a for ^{26}Al, for a ^{26}Al/^{10}Be ratio of 6.85.

The ^{10}Be and ^{26}Al concentrations in the profile can be expressed as Eq. (1):

$$C(x,t) = \frac{P_0 \cdot P_{\text{spallation}}}{\frac{\rho\cdot\varepsilon}{\Lambda_{\text{spallation}}}+\lambda}\cdot e^{-\frac{\rho\cdot x}{\Lambda_{\text{spallation}}}}\cdot\left(1-e^{-\left(\lambda+\frac{\varepsilon\cdot\rho}{\Lambda_{\text{spallation}}}\right)\cdot t}\right) + \frac{P_0 \cdot P_{\text{negative}}}{\frac{\rho\cdot\varepsilon}{\Lambda_{\text{negative}}}+\lambda}\cdot e^{-\frac{\rho\cdot x}{\Lambda_{\text{negative}}}}\cdot\left(1-e^{-\left(\lambda+\frac{\varepsilon\cdot\rho}{\Lambda_{\text{negative}}}\right)\cdot t}\right) + \frac{P_0 \cdot P_{\text{fast}}}{\frac{\rho\cdot\varepsilon}{\Lambda_{\text{fast}}}+\lambda}\cdot e^{-\frac{\rho\cdot x}{\Lambda_{\text{fast}}}}\cdot\left(1-e^{-\left(\lambda+\frac{\varepsilon\cdot\rho}{\Lambda_{\text{fast}}}\right)\cdot t}\right), \quad (1)$$

where P_0 is the total surface production of TCN ($P_{\text{spallation}} = 0.9815$, $P_{\text{negative}} = 0.012$ and $P_{\text{fast}} = 0.0065$), ρ is the density of the regolith (1.6 g/cm^3), ε is the denudation rate, Λ is the effective attenuation lengths of cosmic particles ($\Lambda_{\text{spallation}}$: 160 g/cm^2, $\Lambda_{\text{negative}}$: 1257 g/cm^2, Λ_{fast}: 1988 g/cm^2 [1, 18, 19], x is the sampling depth, and λ is the decay constant of TCNs (^{10}Be: 4.99×10^{-7}/a and ^{26}Al: 9.83×10^{-7}/a) [20, 21].

Because the granite has been exposed at the surface for a long period, it is reasonable to assume that the ^{26}Al and ^{10}Be in the regolith profile have reached a steady state in which neither the topographic form nor the thickness of the regolith changes over time, although erosion removes material from the hillslope [22] and that the concentration

of TCNs has not changed over time. Thus, Eq. (1) can be simplified to Eq. (2):

$$C(x) = \frac{P_0 \cdot P_{\text{spallation}}}{\frac{\rho \cdot \varepsilon}{\Lambda_{\text{spallation}}} + \lambda} \cdot e^{-\frac{\rho \cdot x}{\Lambda_{\text{spallation}}}} + \frac{P_0 \cdot P_{\text{negative}}}{\frac{\rho \cdot \varepsilon}{\Lambda_{\text{negative}}} + \lambda} \cdot e^{-\frac{\rho \cdot x}{\Lambda_{\text{negative}}}} + \frac{P_0 \cdot P_{\text{fast}}}{\frac{\rho \cdot \varepsilon}{\Lambda_{\text{fast}}} + \lambda} \cdot e^{-\frac{\rho \cdot x}{\Lambda_{\text{fast}}}}. \quad (2)$$

In this study, the best-fitting model was calculated using the sum of *Chi*-square (χ^2), as expressed in Eq. (3), to minimize the variance between the theoretical and practical values [3, 23]:

$$\chi^2 = \sum_{i=1}^{N} \left(\frac{Ci - C(x_i)}{\sigma_i} \right)^2, \quad (3)$$

where i represents the sample number, N is the amount of samples in the profile, x_i is the depth of sample i, ε is the denudation rate, t is the exposure time, C_i is the determined concentration of sample i, σ_i is the analytical error at depth x_i, and $C(x_i)$ is the total theoretical cumulative concentration from Eq. (2).

3 Results and discussion

The analytical results are listed in Table 1 and plotted in Fig. 3. The ranges of the measured $^{10}Be/^{9}Be$ and $^{26}Al/^{27}Al$ ratios are $(0.4–6.3) \times 10^{-13}$ and $(0.1–2.1) \times 10^{-12}$, respectively. These values are higher than the process blank samples (typically $<5 \times 10^{-15}$ for both $^{10}Be/^{9}Be$ and $^{26}Al/^{27}Al$); thus, the effect of the blank contribution is not clear. As a result, the ranges of the ^{10}Be and ^{26}Al concentrations are $(2.3–36.6) \times 10^4$ atoms/g and $(1.3–23.1) \times 10^5$ atoms/g, respectively. The $^{26}Al/^{10}Be$ ratios, which range from 5.81–6.59 throughout the profile, are consistent with surface production rates of 6.85 within a 2σ margin of error. This consistency supports the hypothesis that the regolith profile has not undergone burial history.

With the exception of the near-surface sample QHD-1, the ^{10}Be and ^{26}Al concentrations in the deeper samples decrease exponentially with depth; furthermore, they fit Eq. (2). The best fits for ^{10}Be and ^{26}Al result in denudation rates of 8.5 and 9.1 m/Ma, respectively. These values are long-term denudation rates averaged across the 10^4–10^5 a timescale, during which both chemical weathering and physical erosion processes removed a few meters of surface granite rocks. Given a total uncertainty of $\sim$10 %, the denudation rates determined from the ^{10}Be and ^{26}Al profiles are consistent, resulting in an average value of $\sim$9 m/Ma.

Compared with other ^{10}Be and ^{26}Al denudation rates in various lithological, tectonic and climatic areas, the results of this study are significantly lower than the global ^{10}Be mean denudation rate recorded from the basin (218 m/Ma), but similar to the mean erosion rate of its outcrops (12 m/Ma) [6]. Recent research documented that no significant bivariate correlations exist between the basin erosion rate and MAT, MAP, latitude or basin area at the global scale; however, the mean basin slope has a strong positive bivariate correlation with the denudation rate [6]. Figure 4 shows the relationship between the denudation rate of igneous outcrops and MAP in global tropical and temperate areas. The ^{10}Be denudation rates show $\sim$3 orders of magnitude of variation from 0.4 to 134 m/Ma. Compared with other sites, the regolith profile in this study clearly has a relatively lower denudation rate. Tectonic factors are among the major forces that control landscape evolution [2], and the basin slope shows a strong bivariate correlation with the erosion rate [6]. Thus, the flat terrain surrounding the profile (Fig. 1) might be the major determinant of the low denudation rate. Given the field observations, the low denudation rate in Qinhuangdao is attributed to its lack of tectonic activity, which leads to weak physical erosion.

The ^{26}Al and ^{10}Be concentrations in the surface sample QHD-1 are significantly lower than the extrapolation of the theoretical curve deduced from the other five samples (Fig. 3). This offset clearly indicates that the cosmogenic

Table 1 Analytical results of cosmogenic nuclides ^{10}Be and ^{26}Al concentrations in Qinhuangdao granitic profile

Sample ID	Depth (cm)	Quartz (g)	$^{10}Be/^{9}Be$ (10^{-13})	^{10}Be Conc. (10^4 atoms/g)	$^{26}Al/^{27}Al$ (10^{-12})	^{27}Al Conc. (μg/g)	^{26}Al Conc. (10^4 atoms/g)	$^{26}Al/^{10}Be$
QHD-1	5	23.800	6.046 ± 0.209	36.27 ± 1.26	2.065 ± 0.056	1,177	219.35 ± 5.99	6.05 ± 0.27
QHD-2	45	23.265	6.286 ± 0.132	36.63 ± 0.77	2.142 ± 0.055	1,224	230.69 ± 5.99	6.30 ± 0.22
QHD-3	105	23.781	3.512 ± 0.081	21.54 ± 0.50	1.230 ± 0.027	1,165	133.49 ± 2.91	6.20 ± 0.20
QHD-4	175	18.565	1.420 ± 0.072	12.08 ± 0.63	0.469 ± 0.014	1,192	72.62 ± 2.26	6.01 ± 0.37
QHD-5	235	21.657	0.949 ± 0.030	7.47 ± 0.24	0.341 ± 0.012	1,188	49.20 ± 1.77	6.59 ± 0.33
QHD-6	285	18.658	0.402 ± 0.030	2.27 ± 0.19	0.124 ± 0.005	1,160	13.20 ± 0.58	5.81 ± 0.55
Blank	–	–	0.035 ± 0.006	–	0.005 ± 0.002	1,006	–	–

Uncertainties are 1σ

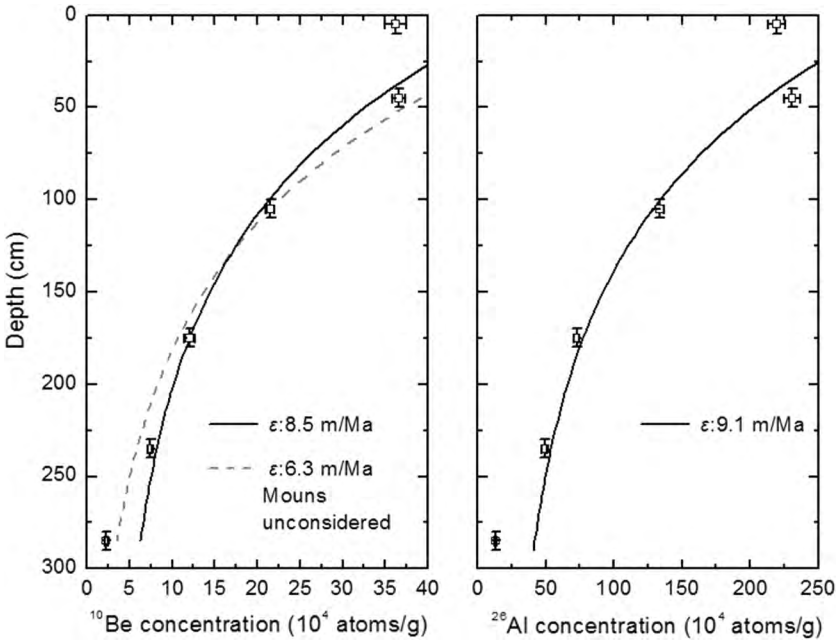

Fig. 3 The ^{10}Be and ^{26}Al depth profile in Qinhuangdao. Error bars indicate 1σ analytical uncertainties. The curves represent the best fitting of steady-state denudation model on the basis of Eq. (2)

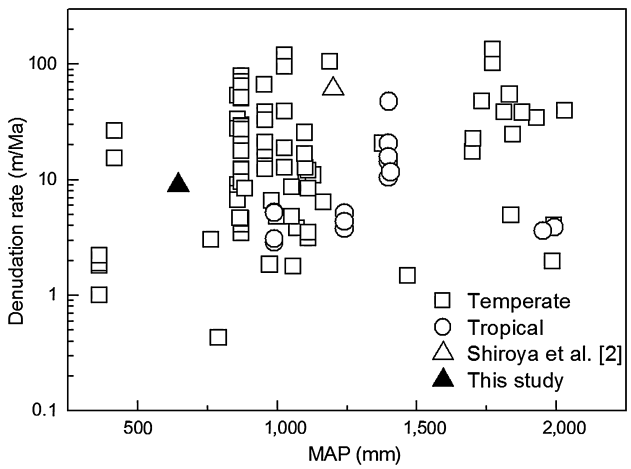

Fig. 4 Relationship between the denudation rate of grantic outcrops and MAP from temperate and tropical areas (data from [2, 6] and references therein)

nuclides in the shallow layer have changed, most likely due to the bioturbation (e.g., plant root, ant and earthworm activity) of the soil layer. A similar phenomenon has been observed elsewhere [24, 25]. By comparing the model fitting result of two surface samples (0–30 cm) with the entire profile dataset (0–190 cm), Shiroya et al. [2] concluded that an accurate determination of the erosion rates of granitic soil surfaces requires the sampling of deeper layers (at least to 80 cm). In addition, quartz enrichment due to the dissolution of other minerals produces calculated error [26, 27] because the concentration of SiO_2 along the profile is between 60 %–70 % lower than that of bedrock 73 % [10]. Thus, the correction factor should be small and within the margin of error. These observations, including those made in this study, imply that the denudation rate determined from river sediment (which is eroded from the soil surface on the basin scale) might be overestimated on occasion. The surface denudation rate calculated from our surface sample QHD-1 is 18 m/Ma, illustrating this possibility.

The sample QHD-6 is slightly lower than the ^{10}Be best-fitting curve in Fig. 3. At present, we lack a convincing explanation for this offset. However, two possibilities should be considered: First, the experimental background subtraction might be overestimated because of the low ^{10}Be concentration; second, the resulting production rates might be overestimated because muons play an important role in producing cosmogenic nuclides in the deeper layer (>3 m). If we assume a smaller contribution from the muons, then the best model fitting seems more apparent and provides a denudation rate of 6 m/Ma. Additional studies of more cosmogenic nuclide depth profiles will help to clarify the alternatives.

4 Conclusions

This study applied a depth profile of the in situ cosmogenic nuclides ^{26}Al and ^{10}Be to determine the long-term denudation rate of a granitic regolith in China. A denudation rate of $\sim$9 m/Ma during the last 10^3–10^5 a was obtained in Qinhuangdao. This result shows a lower denudation rate

than other igneous outcrops. The lack of tectonic activity and the flat terrain are most likely the major factors that control the regolith erosion process. Compared with surface approaches, the depth profile method is more reliable, particularly in cases of surficial soil bioturbation.

Acknowledgments We are grateful to M. Miguens-Rodriguez, A. Rodés and K. Keefe for helping with the experiments. We thank Fan Bailing and Mao Hairuo for their assistance with sample collection. This work was supported by the National Natural Science Foundation of China (41130536, 41210004) and the State Key Laboratory of Environmental Geochemistry, Institute of Geochemistry, Chinese Academy of Sciences (9014).

Conflict of interest The authors declare that they have no conflict of interest.

References

1. Gosse JC, Phillips FM (2001) Terrestrial in situ cosmogenic nuclides: theory and application. Quat Sci Rev 20:1475–1560
2. Shiroya K, Yokoyama Y, Matsuzaki H (2010) Quantitative determination of long-term erosion rates of weathered granitic soil surfaces in western Abukuma, Japan using cosmogenic ^{10}Be and ^{26}Al depth profile. Geochem J 44:23–27
3. Braucher R, Del Castillo P, Sinme L et al (2009) Determination of both exposure time and denudation rate from an in situ-produced ^{10}Be depth profile: a mathematical proof of uniqueness. model sensitivity and applications to natural cases. Quat Geochronol 4:56–67
4. Ferrier KL, Kirchner JW (2008) Effects of physical erosion on chemical denudation rates: a numerical modeling study of soil-mantled hillslopes. Earth Planet Sci Lett 272:591–599
5. Lal D (1991) Cosmic ray labeling of erosion surfaces: in situ nuclide production rates and erosion models. Earth Planet Sci Lett 104:424–439
6. Portenga EW, Bierman PR (2011) Understanding earth's eroding surface with ^{10}Be. GSA Today 21:4–10
7. Huang XT, Zheng HB, Chappell J et al (2013) Characteristics of cosmogenic nuclide ^{10}Be in the yangtze riverine sediments and estimations of erosion rate. Quat Sci 33:671–683 (in Chinese)
8. Kong P, Na CG, Fink D et al (2006) Erosion in northwest Tibet from in-situ-produced cosmogenic ^{10}Be and ^{26}Al in bedrock. Earth Surf Proc Landforms 32:116–125
9. Nutman AP, Wan Y, Du L et al (2011) Multistage late Neoarchaean crustal evolution of the North China Craton, Eastern Hebei. Precam Res 189:43–65
10. Xiong ZF, Gong YM (2006) Geochemical characteristics and climatic-environmental significance of the red weathering crusts in the Beidaihe coast, North China. Earth Sci Front 13:177–186 (in Chinese)
11. Wang JG (2000) Regional geology investigation in Qinhuangdao. China University of Mining and Technology Press, Xuzhou (in Chinese)
12. Zheng LM, Li RQ (1997) Analysis of the neotectonic movement along the sea coast from Qinhuangdao to Cheng Shanjiao in the past 5,000 years. J Beijing Univ Norm (Nat Sci) 33:543–547 (in Chinese)
13. Kohl C, Nishiizumi K (1992) Chemical isolation of quartz for measurement of in situ-produced cosmogenic nuclides. Geochim Cosmochim Acta 56:3583–3587
14. Xu S, Dougans AB, Freeman S et al (2010) Improved ^{10}Be and ^{26}Al ams with a 5 MV spectrometer. Nucl Instr Meth B 268:736–738
15. Granger DE, Riebe CS (2007) Cosmogenic nuclides in weathering and erosion. In: Drever JI (ed) Surface and ground water, weathering, denudation and soils. Treatise on geochemistry, vol 5. Elsevier, London, pp 1–43
16. Stone JO (2000) Air pressure and cosmogenic isotope production. J Geophys Res 105:23753–23759
17. Heisinger B, Lal D, Jull A et al (2002) Production of selected cosmogenic radionuclides by muons: 1. Fast muons. Earth Planet Sci Lett 200:345–355
18. Heisinger B, Lal D, Jull A et al (2002) Production of selected cosmogenic radionuclides by muons: 2. Capture of negative muons. Earth Planet Sci Lett 200:357–369
19. Braucher R, Brown ET, Bourles DL et al (2003) In situ produced ^{10}Be measurements at great depths: implications for production rates by fast muons. Earth Planet Sci Lett 211:251–258
20. Chmeleff J, Von Blanckenburg F, Kossert K et al (2010) Determination of the ^{10}Be half-life by multicollector ICP-MS and liquid scintillation counting. Nucl Instr Meth B 268:192–199
21. Nishiizumi K (2004) Preparation of ^{26}Al AMS standards. Nucl Instr Meth B 223:388–392
22. Gilbert GK (1909) The convexity of hilltops. J Geol 17:344–350
23. Siame L, Bellier O, Braucher R et al (2004) Local erosion rates versus active tectonics: cosmic ray exposure modelling in Provence (south-east France). Earth Planet Sci Lett 220:345–364
24. Perg LA, Anderson RS, Finkel RC (2001) Use of a new ^{10}Be and ^{26}Al inventory method to date marine terraces, Santa Cruz, California, USA. Geology 29:879–882
25. Gabet EJ, Reichman OJ, Seabloom EW (2003) The effects of bioturbation on soil processes and sediment transport. Annu Rev Earth Planet Sci 31:249–273
26. Small EE, Anderson RS, Hancock GS (1999) Estimates of the rate of regolith production using ^{10}Be and ^{26}Al from an alpine hillslope. Geomorphology 27:131–150
27. Riebe CS, Kirchner JW, Granger DE (2001) Quantifying quartz enrichment and its consequences for cosmogenic measurements of erosion rates from alluvial sediment and regolith. Geomorphology 40:15–19